SCANNING Vol. 14, 325–333 (1992)

Received August 14, 1992

Light Transport in Single-Crystal Scintillation Detectors in SEM

P. Schauer and R. Autrata

Department of Electron Optics, Institute of Scientific Instruments, Czechoslovak Academy of Sciences, Brno, Czechoslovakia

Summary: A Monte Carlo simulation method was developed to determine the efficiency of photon transport through a modified rotationally symmetric Everhart-Thornley detector. The method makes use of the random generation of photon emission from a luminescent centre and describes the trajectory of photons and the efficiency of their transport toward the photocathode of the photomultiplier tube. The model includes photon generation in a point source, mirror reflection by a metal-coated surface, Fresnel reflection by a metal-uncoated surface, Fresnel passage through the boundary of different materials, diffusion reflection, and passage through a matted surface and optical absorption in material. For the simulation, an IBM-PC-compatible program was written and applied to detection systems with disc, conical, and hemispherical YAG:Ce single-crystal scintillators with cylindrical or tapered light guides or without any light guide. The model was verified by measuring the efficiency of detection systems excited by the primary electron beam in the line-scan SEM mode.

Introduction

In SEM, the most frequently used detector for signal electrons is the Everhart-Thornley (ET) scintillation detector (Everhart and Thornley 1960). Its efficiency influences the signal-to-noise ratio (SNR) of the resulting image, especially for low values of currents of the exciting beam. While much attention has been paid to the efficiency of the energy conversion (electron photon) in the scintillator (Autrata *et al.* 1983, Pawley 1974, Robbins 1980), the processing of signal photons with minimum losses has been neglected.

The wider use of single-crystal scintillation materials (Autrata *et al.* 1978, 1983a, 1983b, Shmulovich *et al.* 1988), while raising new possibilities, also brought to light new problems associated with an efficient transport of signal photons through the detection system (scintillator and light guide) toward the photocathode of the photomultiplier (PMT). The optimum design of the light guide system depends on the proper choice of material of the scintillator and light guide, as well as on their geometry. An additional factor is the kind of treatment of all parts of their surfaces, including boundaries between the individual component parts (scintillator–light guide–PMT) of the ET detector. For example, the matted surface of the output area of the disc scintillator need not be suitable for a scintillator of some other geometry. Application of the transparent conductive indium-tin-oxide (ITO) layer to the surface of the hemispherical scintillator need not be appropriate for a similar system with a conical scintillator. It is even more difficult to choose a suitable material, geometry, and surface treatment when tapered or broadened light guides are used.

The design of the detection system must comply with the space available in the microscope, and at the same time the maximum efficiency of the transport of signal photons toward the photocathode of the PMT must be maintained. Estimation of optical properties of the ET detector, its production and experimental verification is a very time-consuming task. It is also an expensive method and subject to failure. It is therefore very advantageous to design the ET detector after a quantitative optical analysis has been made.

Quantitative optical analysis of the ET detector can be carried out analytically (Carrier and Lecomte 1990a, Keil 1970). The advantage of this method is the quick and easy obtainment of results when dimensions and optical parameters are changed. However, if the analytical expression is not to be too complex, the system geometry must show a very high symmetry. A method which makes use of Monte Carlo simulation (Carrier and Lecomte 1990b, Xiaoguang 1984) is more generally applicable. It does not depend on the symmetry of the simulated systems, and if one can restrict the simulation to rotationally symmetric detection systems, the photon transport in the detector can be expressed in a quite simple way. The disadvantages of this method are that it is feasible only by using a computer and that it may require more time.

Address for reprints:

P. Schauer
Institute of Scientific Instruments
Czechoslovak Academy of Sciences
Královopolská 147
CS-612 64 Brno, Czechoslovakia

In this article, a Monte Carlo method was chosen for the comparison of the efficiency of photon transport in detection systems. The results of the optical analysis of the scintillation detector will be expressed by the so-called transport efficiency of the scintillation detector. This quantity gives the efficiency of transport of photons toward the photocathode of the PMT in dependence on the point of excitation on the scintillator surface. In fact, it is a function of one variable coordinate for rotationally symmetric detection systems and a function of two variable coordinates for other systems, because one coordinate depends on the others according to the scintillator surface geometry. The mean value of this function gives the mean transport efficiency of the detector.

Monte Carlo Simulation

The Monte Carlo (MC) method makes use of random generation of photon emission from a luminescent centre and describes the trajectory and the efficiency of the transport of a photon as far as the photocathode of the PMT. Repeated generation of the trajectory many times (1,000–10,000 times) makes it possible to determine the efficiency of light transfer from the given position of generation (point of excitation by primary electrons) at the scintillator surface. If the coordinates and directional cosines of the photon are recorded at the end of each trajectory, further quantitative information, for example, about the light intensity distribution and about the direction of light propagation at the photocathode of the PMT can be obtained using this simulation method. The sequence of the following physical processes was included in the simulation computer program:

Generation of a photon takes place in the point source. The propagation of the photon is isotropic. The initial directional cosines C_x, C_y, and C_z of each trajectory are random and are determined by two random numbers R_1 and R_2 from the interval [0,1] as follows:

$$\begin{aligned} C_x &= D\cos(2\pi R_1), \\ C_y &= D\sin(2\pi R_1), \\ C_z &= \pm D\cos\left[\frac{\pi}{2} - \arccos(1-2R_2)\right], \\ C_x^2 &+ C_y^2 + C_z^2 = 1, \end{aligned} \tag{1}$$

where, D is the coefficient given by the last equation. $C_z \geq 0$ for $R_2 \leq ½$ and $C_z < 0$ for $R_2 > ½$.

Each step of the photon trajectory is given by the abscissa between two subsequent interactions of the photon with the scintillator or light guide surfaces. After each step, a new direction of the trajectory and a new probability that the photon will reach the photocathode of the PMT are determined. This probability is calculated from the losses that occur within the volume and on the surface of the active material.

The position of interaction of the photon with the surface of the scintillator or light guide is found as the point of intersection of the photon trajectory and the nearest surface of the rotationally symmetric body which satisfies the boundary conditions of the delimited surface. All surfaces are described by the same equation:

$$k_x \frac{x^2}{A^2} + k_y \frac{y^2}{B^2} + k_z \frac{(z-z_0)^2}{C^2} = P \tag{2}$$

where x, y, and z are coordinates of the point of intersection, z_0 ($x_0 = y_0 = 0$) are coordinates of the centre or of the apex of the body, and k_x, k_y, k_z, A, B, C, and P are coefficients of the lateral areas which are different for different bodies, and they are presented in Table I. Axis z is the axis of symmetry of the detection system.

Photon absorption in the volume of the material is determined by the absorption coefficient α of each material used. The determination of each abscissa of the photon trajectory (n-th step) is followed by the evaluation of the probability $p_n = \exp(-\alpha l_n)$ with which the photon will travel along the path l_n of this line segment. This probability is immediately included into the new probability that the photon will reach the photocathode of the PMT.

Mirror reflection from a metal-coated surface is determined by the constant coefficient of reflectivity r of each active surface. The probability that the photon will be reflected by the coated surface in the direction determined by the law of mirror reflection is equal to r. After the reflection has been completed, this probability is immediately included into the new probability that the photon will reach the photocathode of the PMT.

Fresnel reflection or passage through a polished surface is determined by the Fresnel formula (Billings 1972). Equality of parallel and perpendicular polarization, and mirror reflection are assumed:

$$\begin{aligned} R &= \frac{1}{2}\left[\frac{\sin^2(\beta_1-\beta_2)}{\sin^2(\beta_1+\beta_2)} + \frac{\tan^2(\beta_1-\beta_2)}{\tan^2(\beta_1+\beta_2)}\right], \\ T &= 1-R \end{aligned} \tag{3}$$

Here, R is the coefficient of reflectivity and T is the coefficient of transmissivity of the boundary. β_1 is the angle of incidence and β_2 is the angle of refraction for which $n_1\sin\beta_1 = n_2\sin\beta_2$, where n_1 and n_2 are indices of refraction of the medium of incidence and of the medium of refraction, respectively. How the trajectory will further be shaped depends on whether the photon will be reflected or refracted by the active surface. For the peripheral light-guiding surface (which is intended for reflection), the trajectory always exhibits reflection. For the surface that serves as the boundary between the neighbouring light-guiding elements of the system (which is intended for transmission), the trajectory exhibits reflection only when the condition of total internal reflection is fulfilled. The probability that the photon will be reflected and refracted to the photo-

TABLE I Coefficients of Eq. (2) for different lateral areas[a]

Body/coefficient	*A*	*B*	*C*	k_x	k_y	k_z	P
Sphere	r_s	r_s	r_s	1	1	1	1
Cone	r_c	r_c	v	1	1	−1	0
Cylinder	r_c	r_c	1	1	1	0	1
Circular plane	r_c	r_c	1	0	0	1	0
Ellipsoid	a	a	c	1	1	1	1
Hyperboloid	a	a	c	1	1	−1	1
Paraboloid	r_c	r_c	1	1	1	−1	0

[a] Key: r_s is the sphere radius; r_c is the circular base radius; a is the length of the half-axis in the plane of symmetry; c is the length of the half-axis along the axis *z*; v is the cone height.

cathode is equal to *R* and to *T*, respectively. After every interaction of the photon with the polished surface, this probability is included into a new total probability which assumes that this photon will reach the photocathode of the PMT.

Diffusion reflection or passage through the matted surface is described using a randomly chosen number R_3 that will determine the direction of the normal of the plane of the boundary for every interaction of the photon with the diffused surface. The remaining actions of the photon are simulated using the algorithm identical with that for the polished surface.

The photon trajectory is terminated at the photocathode of the PMT only if the probability that the photon will reach the photocathode is greater than 10^{-8}. If in any step of the trajectory the probability that the photon will reach the photocathode drops below the mentioned value, the photon is considered as lost. Zero probability that the photon reaches the photocathode is ascribed to the said photon and the simulation of this trajectory is immediately stopped. After terminating the trajectory, the probability that the photon will reach the surface of the photocathode is ascribed to the mean value obtained for the preceding trajectories (for photons emitted from the same point) and the generation of another photon is started. This mean value continuously determines the efficiency of the transport of the photon through the detection system.

Detection System Configuration

Figure 1a–c shows geometrical configurations of scintillators and light guides for which the simulation program was used. Scintillator — light guide systems of the ET detector consisting of a single crystal scintillator (disc, cone, or hemisphere) in the combination with a cylindrical or tapered light guide were tested. The tapered cylindrical light guide was additionally tested in connection with the fibre light guide (Fig. 1c). The simulation of the photon transport through the fibre light guide was simplified to the transport through one fibre, so that losses for the photon picked up outside the light guide core were neglected. The dimensions are summarised in Table II.

TABLE II Simulation parameters and experimental conditions

Index of refraction:	Scintillator	1.84
	Bulk light guide	1.49
	Fibre light core	1.60
	Fibre light guide cladding	1.50
	Optical cement	1.56
	ITO	2.05
Absorption: (mm^{-1})	Scintillator	0.0743
	Bulk light guide	0.000816
	Fibre light guide core	0.00254
	Optical cement	0.00120
	ITO	0.0009
Reflectivity:	good Al	0.80
	bad Al	0.50
Dimensions: (mm)		
Height:	Disc scintillator	0.5
	Cone scintillator	1.5
Diameter:	Scintillator base	12.3
	Cylindrical light guide	12.6
	Tapered light guide	12.6/7.0
	Fibre light guide	7.0
Length:	Cylindrical light guide	35.0
	Tapered light guide	35.0
	Fibre light guide	400.0
Number of photons investigated		1,000

The YAG:Ce single-crystal, polymethyl methacrylate (PMMA) and glass were materials used for scintillators, compact light guides, and the fibre light guides, respectively. Vacuum deposited aluminium and indium tin oxide (ITO) were used as metal and transparent conductive scintillator coatings, respectively. The properties of the materials used are summarised in Table II.

The photon transport efficiency was simulated for different shapes and different kinds of surface treatment of a solo scintillator (no light guide used) (Fig. 1a) and of a system consisting of a scintillator and light guide (Fig. 1b, 1c). The input surface of the scintillator, i.e., the area through which signal electrons enter the scintillator, must always be conductive. Therefore, it was simulated as a surface coated with an Al or ITO layer. The remaining areas of the scintillator or light guide, with the exception of the

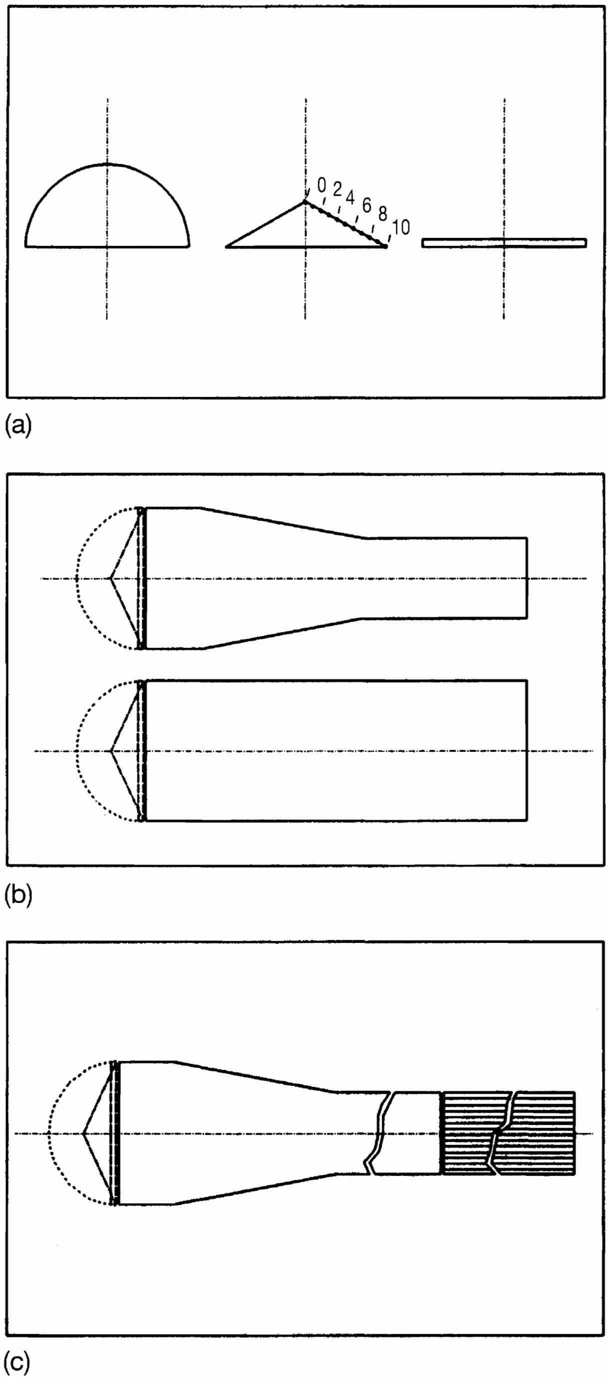

FIG. 1 Geometry of scintillators and of bulk and fibre light guides. (a) Three alternative shapes of single crystal scintillators. Points of electron impact are indicated only for the cone-shaped scintillator. (b) Two alternative (cylindrical or tapered) bulk light guides with indicated alternative types of scintillators. (c) Combined system containing bulk (tapered) and fibre light guide.

output surface of the scintillator (the surface connected to the input surface of the light guide or to the entrance window of the PMT), were simulated as ideally smooth areas. Three kinds of surface treatment of the output area of the scintillator were considered: (1) polished surface when no optical cement was used, (2) polished surface when an optical cement was used, and (3) matted surface when no optical cement was used.

Results of Simulation and Discussion

All detection systems investigated were rotationally symmetric so that the efficiency of the photon transport through the system in dependence on the point of excitation also showed rotational symmetry. It was therefore sufficient to simulate the transport efficiency for the points of excitation along the radial curve of the input surface of the scintillator. For all systems tested, 11 uniformly distributed points (points of impact of the excitation electron) were chosen along this radial curve (Fig. 1a). Point number 0 always lay on the axis of symmetry and point number 10 close to the periphery of the input surface of the scintillator.

The computations were running using a 16 MHz PC/286. The program was written in FORTRAN 77. The efficiency of transport of 1000 photons from every point of excitation was simulated. The computation of these 1000 trajectories took 30 seconds to 25 minutes, depending on the efficiency and the complexity of the simulated configuration.

The detection systems containing a scintillator can be divided into two groups, depending on the absence or presence of the light guide. Of the former group, such detection systems are interesting for applications in SEM, the scintillator of which is positioned directly on the entrance window of PMT or is even part of this window. Such prospective scintillation detection systems are not yet commercially available. To test the detection efficiency of systems using no light guide, MC simulation of solo scintillators was carried out. The plot of the transport efficiency of the solo scintillators versus the electron impact point number for different kinds of treatment of the input and output surfaces of the single-crystal scintillator is shown in Figure 2a, b.

Electron impact point number N is dimensionless, and it expresses the *relative* position of electron impact. In the program, used for a calculation of light transport through the detection system, the "input" surface of a scintillator is divided into a representative set of numbered points. For rotationally symmetric scintillators, the points are distributed radially and the radius r (distance from axis) of each electron impact point may be calculated as:

$$r = N\,\frac{R}{10},$$

where R is the radius of scintillator. There is, at least, one reason for the introduction of this point number N. The radial dependence of the transport efficiency can be drawn in the same graph, even if diameters of compared scintillators are considerably different.

Detection systems containing light guides are used mostly in SEM because they allow a large variety of spatial configurations in the specimen chamber. The results of MC sim-

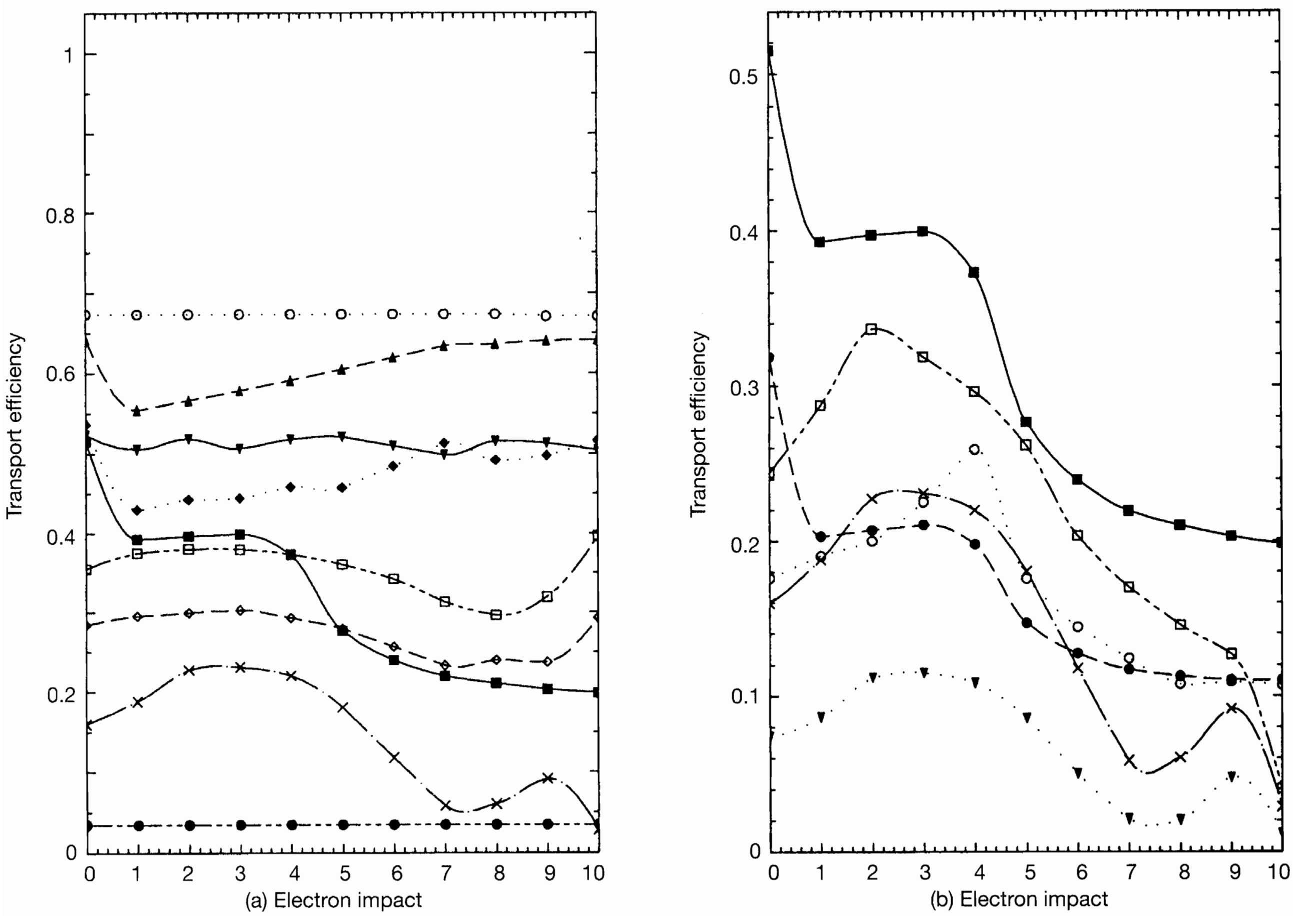

FIG. 2 Dependence of the transport efficiency on the radial position of the electron impact point for scintillators without any light guide. If not otherwise specified, surfaces are polished, no optical cement is used, and good Al (80% reflectivity) is supposed to be deposited on the input surface. (a) The effect of the output surface treatment. Solo YAG: Ce scintillators: ○ disc with cement; –▲– cone with cement; –▼– disc, matted output; –◆– cone, matted output; –■– polished cone; –□– hemisph. with cement; –◇– hemisph., matted out; –×– polished hemisphere; –●– polished disc; (b) The effect of the input surface treatment. If bad AL is used, 50% reflectivity is supposed. Polished Solo YAG: CE scintillators: –■– cone with good Al; –□– hemisphere with ITO; –○– cone with ITO; –×– hemisphere with good Al; –●– cone with bad Al; ▼ hemisphere with bad Al.

ulation of the transport efficiency of detection systems with the cylindrical, tapered, and combined tapered and fibre light guides are shown in Figures 3, 4, and 5, respectively.

Systems with Disc Scintillators

It follows from the results of simulation (Fig. 2a) that polished single-crystal disc scintillators have a lower efficiency than the other types with a lower symmetry. A polished single-crystal disc scintillator showed transport efficiency lower than 0.05. Simulation proved that the light must be guided from the polished disc scintillators toward the light guide or toward the photocathode of PMT by using optical cement. The transport efficiency of the polished disc itself (without light guide!) then increases to nearly 0.7. However, this arrangement is not sufficient if a light guide is used, (Fig. 3), because the photons move in a direction contrary to form, so that most of them are lost on the lateral area of the light guide.

If a disc scintillator is to be used in system with a light guide, it is more advantageous to grind its output surface area to a matte finish and to use no optical cement. Compared with a polished surface scintillator, this scintillator has a lower transport efficiency (it decreased from 0.67 to 0.50, Fig. 2a), but in connection with the cylindrical light guide, its transport efficiency is acceptable (higher than 0.18, Fig. 3). However, if a disc scintillator with a matte output surface is used in a system containing a tapered light guide, the transport efficiency decreases to less than 0.018, and if the light guide is combined with a fibre light guide, it decreases to 0.0018 (see Figs. 4 and 5).

Systems with Cone-Shaped Scintillators

The advantages of cone-shaped scintillators become evident when a detector transport efficiency higher than 0.2 is to be achieved. Monte Carlo simulation has shown that the mean transport efficiency of a system consisting of cone-

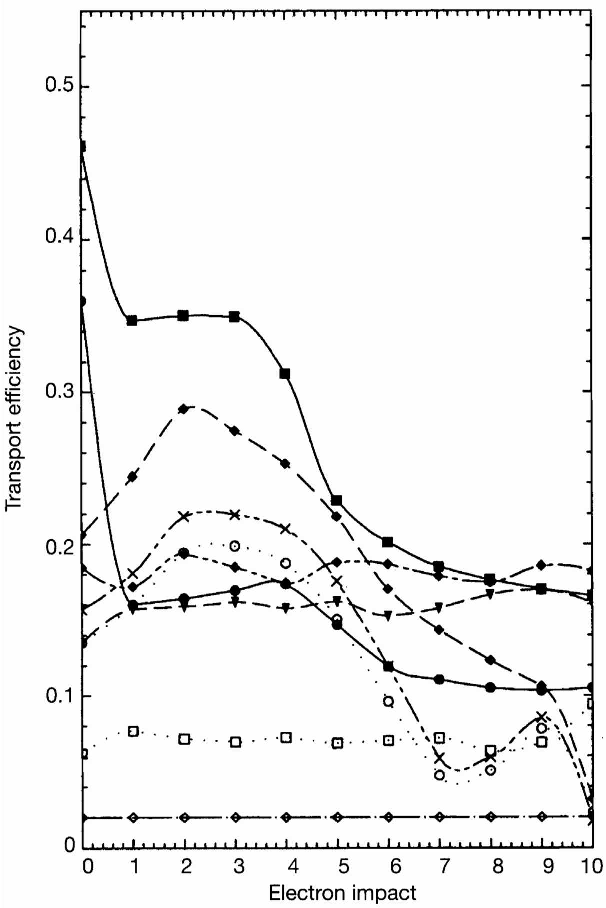

FIG. 3 Dependence of the transport efficiency on the radial position of electron impact point for scintillators with cylindrical light guides. If not otherwise specified, surfaces are polished and good Al and no optical cement are used. If optical cement is used, it is applied only to the scintillator – light guide boundary. YAG: Ce with cylindrical light guide: -■- cone with A1; -♦- hemisphere with ITO; -×- hemisphere with A1 and cement; -○- hemisphere with A1; -♦- disc with matted output; -●- cone with A1 and cement; -▼- cone with matted output; -□- hemisphere with matted output; -◇- disc with A1 and cement.

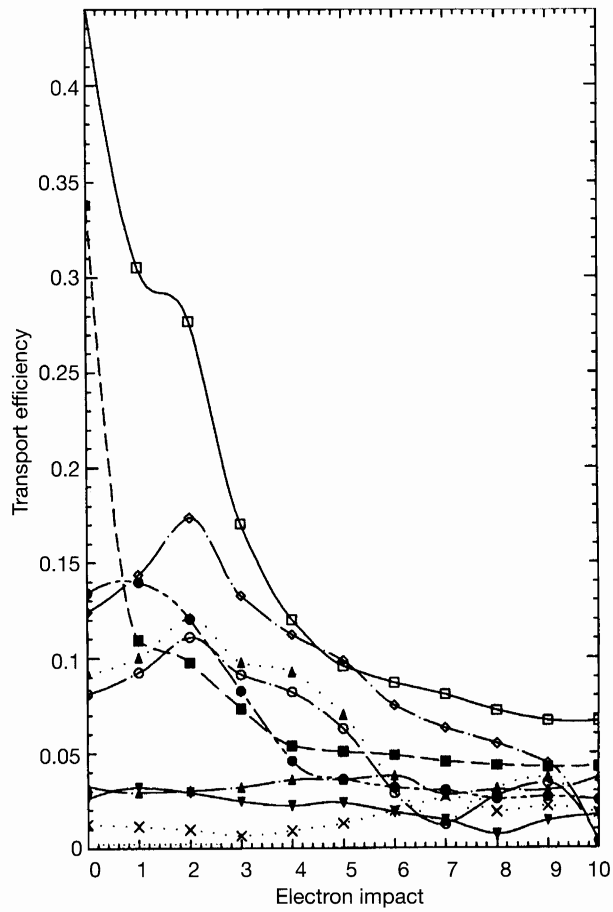

FIG. 4 Dependence of the transport efficiency on the radial position of electron impact point for scintillators with tapered light guides. If not otherwise specified, surfaces are polished and good Al and no optical cement are used. If optical cement is used, it is applied only to the scintillator – light guide boundary. YAG: Ce with tapered light guide: -□- cone with A1; -◇- hemisphere with ITO; -●- cone with ITO; -▲- hemisphere with A1 and cement; -○- hemisphere with A1; -■- cone with A1 and cement; -▲- cone with matted output; -▼- hemisphere with matted output; -×- disc with matted output.

shaped scintillator and a cylindrical light guide amounts to 0.22 (Fig. 3, curve with full square marks). If no light guide is used, it is better to apply cement to the output area of cone-shaped scintillator. However, if the optical cement is applied to a cone-shaped scintillator connected to the light guide, the transport efficiency of the system decreases to one half or even one seventh, depending on the type of scintillator used (Figs. 3, 4, and 5).

The disadvantage of a system containing a cone-shaped scintillator is a marked planar inhomogeneity of the transport efficiency. The transport efficiency steeply decreases as the point of excitation moves from the top to the periphery of the scintillator cone, as evident from Figure 2b (and also from Figs. 3, 4, and 5). If conditions are created such that the signal electron is allowed to be incident on the area near the top of the cone (Autrata 1990), it is possible to increase the transport efficiency of the system 2 to 5 times, depending on the type of light guide used.

The planar homogeneity and the mean value of the transport efficiency of a system with a cone-shaped scintillator can be influenced by the choice of the apex angle of the cone. A change in the apex angle of the cone causes a change in the direction of travel of photons which occurs at the place where they enter the light guide. For different types of light guides, the optimum apex angle is different. The geometry of the cone-shaped scintillator was optimized for the tapered light guide as shown in Figure 1b.

The planar homogeneity of transport efficiency can be markedly increased if the output surface of the cone-shaped scintillator is matted by grinding. In this case, however, the mean transport efficiency decreases below the

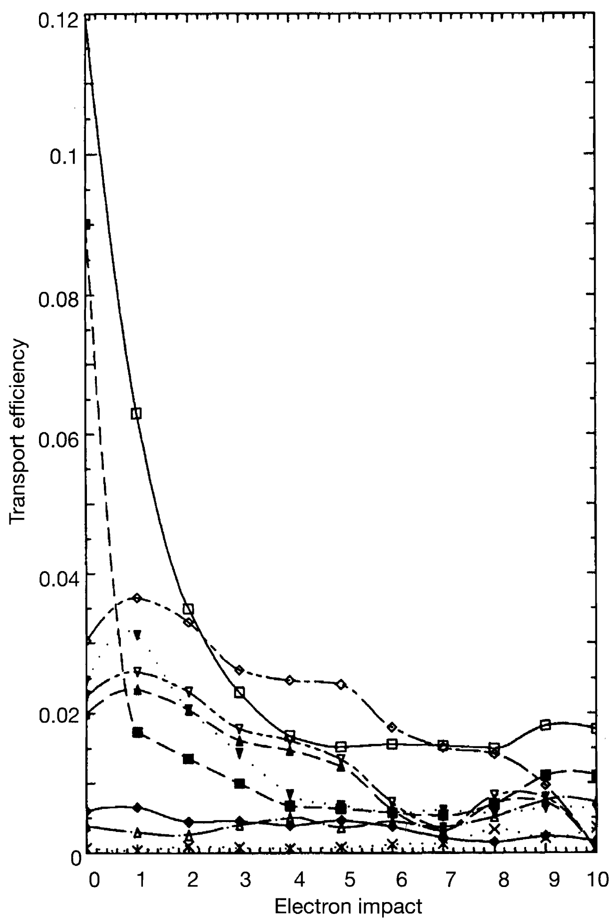

FIG. 5 Dependence of the transport efficiency on the radial position of electron impact point for scintillators with combined (tapered and fibre) light guides. If not otherwise specified, surfaces are polished and good Al and no optical cement are used. If optical cement is used, it is applied only to the scintillator – light guide boundary. YAG: Ce with tapered and fibre LGs: –□– cone with A1; –■– cone with A1 and cement; –◆– hemisphere with ITO; –▼– cone with ITO; ∇ hemisphere with A1 and cement; –▲– hemisphere with A1; –◆– hemisphere with matted output; △ cone with matted output; –×– disc with matted output.

level of similar systems with disc scintillators. Therefore, such a treatment is of no practical significance.

Systems with Hemispherical Scintillators

The planar homogeneity is increased if a system with a hemispherical scintillator is used. The importance of this statement increases with increasing complexity of the light guide system used. Further, it holds that the transport efficiency of the system is higher when the excitation takes place near the axis of symmetry, but, for complex detection systems with tapered and fibre light guides (Fig. 5), the differences in the transport efficiency are not as great as for systems with cone-shaped scintillators. Their mean transport efficiency is about half that of similar systems with cone-shaped scintillators (for a system with a cylindrical light guide it amounts to 0.10). From this it follows that if a higher planar homogeneity is requested, then it is more advantageous to use systems with hemispherical scintillators.

It is suitable to apply optical cement to the output surface of the hemispherical scintillator. The transport efficiency of the system is then increased by approximately 10%. Unlike the systems with cone-shaped scintillators, the output surface of the hemispherical scintillator has no effect on the direction of propagation of the photon toward the light guide. As in the case of the cone-shaped scintillators, it is also unsuitable to mat the output surface of the hemispherical scintillators (connected to the light guides). The matted surface would increase the planar homogeneity, but at the expense of the decrease in the mean value of the transport efficiency to two thirds or even one third.

Treatment of the Conductive Surface of the Scintillator

The surface through which the signal electrons enter the scintillator should be electrically conductive to prevent the generation of a surface charge and it should have a high internal optical reflectivity to ensure an efficient collection of the generated photons. If a conductive film is used, it must transmit excitation electrons over a wide range of energies.

In practice, a thin aluminium coating is usually used. The advantage is that its reflectivity is nearly independent of the photon impact direction. However, the disadvantage is that for a conventional good coating (50 nm thick) the value of the reflectivity is as low as ca. 80%. Bad aluminium coatings or old coatings have even a markedly lower reflectivity (< 50%). As is obvious from Figure 2b, the results of simulation show that the coating has an approximately equal effect on the transport efficiency of the cone-shaped and hemispherical scintillators. Owing to a bad aluminium coating, the efficiency decreases to approximately one half. This proves that the input surface strongly influences the transport efficiency of the detector and attention must therefore be paid to its treatment.

The thin aluminium coating can be replaced by a transparent conductive indium tin oxide (ITO) layer. ITO possesses a high index of refraction and it therefore shows nearly 100% reflectivity for a great number of photons for which the trajectories satisfy the demand of total reflection, but, on the contrary, it shows a very low reflectivity for the photons moving in other directions. This can be of advantage if photons move near the input surface where the interaction of the photon with the surface often occurs and when the angle of incidence is high as, for example, in the hemispherical scintillator. It follows from the results of simulation shown in Figure 2b that the replacement of a good aluminium coating by an ITO layer results in an approximately 1.5-fold increase in the transport efficiency of the hemispherical scintillator. For other detection systems with hemispherical scintillators investigated (Figs. 3, 4, and 5), this increase is even somewhat higher. With cone-shaped scintillators where photons do not move along the entrance surface, especially when excitation takes place near the tip of the cone, the replacement of the aluminium coating by an ITO layer causes a decrease in the mean transport efficiency. This decrease amounts to one half or even one third, depending on the type of light guide used.

Experimental Verification

The MC simulation model was verified using a Tesla BS 340 SEM in the line-scan mode (Autrata 1990). A primary electron beam with an energy of 10 keV and a current of 110 pA was incident on the radial of the surface of the scintillator. YAG:Ce single crystal scintillators were used. Their geometries and dimensions are shown in Figure 1 and Table II, respectively. The restricted space of the specimen chamber allowed only the measurement of detection systems with fibre light guides similar to those illustrated in Figure 1c. The tapered light guide was prepared from PMMA. Carl Zeiss Jena fibre light guides were adapted for use in vacuum.

The results of experiments for systems with disc scintillators with a matted output surface, polished hemispherical scintillators, and polished cone-shaped scintillators are shown in Figure 6a-c, respectively. The photographs represent the intensity of the output signal from the PMT radially distributed on the scintillator surface. The maxima for cone-shaped and hemispherical scintillators correspond to the axis point of the scintillator.

The results of simulation for the corresponding detection systems are shown in Figure 7. Their configuration was practically identical with that of the systems shown in Figure 5. The only difference was that the configuration comprised also the ring fixing the scintillator to the light guide. The ring did not affect the properties of the scintillator, but influenced only the reflectivity of that cylindrical lateral area of the light guide with which it was in contact. It is obvious that the results are in a good agreement with the experimental ones shown in Figure 6. Even the experimentally found slight increase in the transport efficiency of the system with the disc scintillator which takes place in the direction towards the disc edge is in a good agreement with the result obtained by simulation.

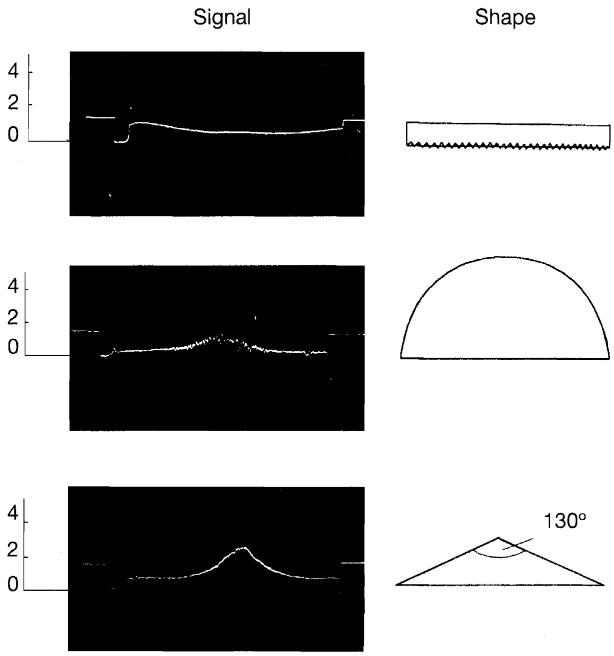

FIG. 6 Line-scan cathodoluminescence of different shapes of YAG:Ce single crystal scintillators. (a) Disc with matted output, (b) polished hemisphere, and (c) polished cone. The maxima of second and third shape correspond to the axis point of the scintillator (point number 0).

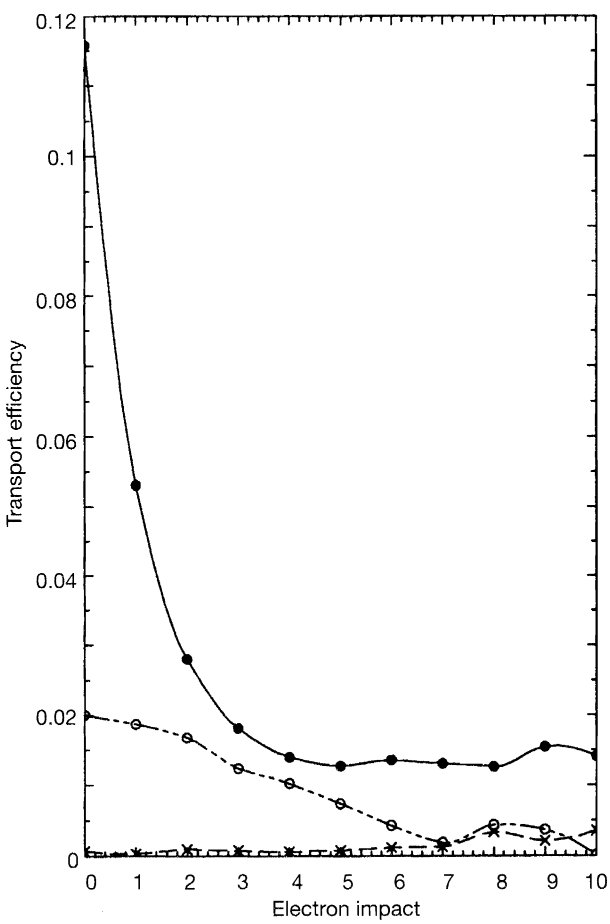

FIG. 7 Comparison of the MC model with the experiment. Dependence of the transport efficiency on the radial position of electron impact point for scintillators with combined light guides and a fixing ring. Good Al is supposed to be deposited on the input surface of the scintillator. No optical cement is used. If not otherwise specified, surfaces are polished. YAG: Ce with combined LG and fixing ring –●– cone with Al; –○– hemisphere with Al; –×– disc with Al and matted output.

Conclusions

Monte Carlo simulation of the transport efficiency of detection systems is a reliable, very fast, and cheap method of designing detectors for signal electrons for SEM. For rotationally symmetric detection systems the following conclusions can be drawn:

(1) For detectors without light guides it is most advantageous to use a disc scintillator and optical cement. The use of a solo hemispherical scintillator is not advantageous. (2) For detection systems with light guides, a cone shaped scintillator is suitable if the planar signal homogeneity is not important. If it is important, then the hemispherical scintillator is more convenient. (3) The transport efficiency of systems with cone-shaped scintillators must be optimized by the proper choice of the apex angle of the cone. (4) If the disc scintillator is connected to the light guide, its output surface must be matted. However, the efficiency of this system is lower than that of systems with other shapes of scintillators. (5) An imperfect reflective layer on the scintillator surface influences significantly the transport efficiency of the whole detection system. (6) With a hemispherical scintillator, it is advantageous to replace the conductive aluminium coating by the ITO layer.

Acknowledgments

The authors thank Dr. Jiří Kvapil, Dr. Josef Kvapil and Mr. K. Blažek from Monokrystaly Turnov for supplying the YAG single crystal scintillators. They also thank Mrs. L. Pohanková for her assistance during compiling of this manuscript.

References

Autrata R: A modification of the ET secondary electron detector with a single crystal scintillator. *Scanning* 12, 119–125 (1990)

Autrata R, Schauer P, Kvapil Jo, Kvapil Ji: Single crystal of YAG—new fast scintillator in SEM. *J Phys E: Sci Instrum* 11, 707–708 (1978)

Autrata R, Schauer P, Kvapil Jo, Kvapil Ji: Cathodoluminescent efficiency of $Y_3Al_5O_{12}$ and $YAlO_3$ single crystals in dependence on Ce^{3+} and other dopants concentrations. *Cryst Res Technol* 18, 907–913 (1983a)

Autrata R, Schauer P, Kvapil Jo, Kvapil Ji: Single-crystal aluminates—a new generation of scintillators for scanning electron microscopes and transparent screens in electron optical devices. *Scanning Electron Microscopy 1983/II*, SEM Inc., AMF O'Hare, Chicago, (1983b) 489–500

Billings BH: In *American Institute of Physics Handbook*. Section 6: *Optics*, 3rd ed. (Ed. Grey DE). McGraw-Hill, New York (1972)

Carrier C, Lecomte R: Trapping of fluorescent light in cylindrical scintillators. *Nucl Instrum Methods Phys Res* A278, 622–624 (1989)

Carrier C, Lecomte R: Theoretical modelling of light transport in rectangular parallelepipedic scintillators. *Nucl Instrum Methods Phys Res* A292, 685–692 (1990a)

Carrier C, Lecomte R: Effect of geometrical modifications and crystal defects on light collection in ideal rectangular parallelepipedic BGO scintillators. *Nucl Instrum Methods Phys Res* A294, 355–364 (1990b)

Everhart TE, Thornley FM: Wide-band detector for micro-microampere low energy electron currents. *J Sci Instrum* 37, 246–248 (1960)

Keil G: Design principles of fluorescence radiation converters. *Nucl Instrum Methods* 87, 111–123 (1970)

Pawley J: Performance of SEM scintillation materials. *Scanning Electron Microscopy*, IITRI, Chicago, (1974) 27–34

Robbins DJ: On predicting the maximum efficiency of phosphor systems excited by ionizing radiation. *J Electrochem Soc* 127, 2694–2701 (1980)

Shmulovich J, Berkstresser GW, Brandle CD, Valentino A: Single-crystal rare-earth-doped yttrium orthosilicate phosphors. *J Electrochem Soc* 135, 3141–3151 (1988)

Xiaoguang Y: A study of light collection efficiency in scintillation detectors. *Nucl Instrum Methods Phys Res* 228, 101–104 (1984)